Journal of Experimental and Theoretical Physics, Vol. 90, No. 5, 2000, pp. 769–777.
From Zhurnal Éksperimental'noĭ i Teoreticheskoĭ Fiziki, Vol. 117, No. 5, 2000, pp. 885–894.

ATOMS, SPECTRA, RADIATION

Towards the Fluorescence Resonance Energy Transfer (FRET) Scanning Near-Field Optical Microscopy: Investigation of Nanolocal FRET Processes and FRET Probe Microscope¶

S. K. Sekatskiĭ*, *, G. T. Shubeita*, M. Chergui*, G. Dietler*, B. N. Mironov**, D. A. Lapshin**, and V. S. Letokhov****

**Institut de Physique de la Matiére Condensée, Université de Lausanne, CH-1015, Lausanne-Dorigny, Switzerland*

***Institute of Spectroscopy, Russian Academy of Sciences, Troitsk, Moscow oblast, 142092 Russia*

****e-mail: sekats@lls.isan.troitsk.ru*

Received November 30, 1999

Abstract—The fluorescence resonance energy-transfer (FRET) process is investigated between donor dye molecules deposited on the sample surface and acceptor dye molecules deposited on the tips of scanning near-field and atomic force microscopes. The FRET process was observed only when the tip acquired contact with the sample and took place in regions of sizes of only a few tens of nanometers with only a few thousands (or even hundreds) of molecules involved. The dependence of the FRET intensity on the tip-sample acting force is recorded and interpreted. In relation to the obtained results, the construction of a previously proposed one-atom FRET SNOM is described. © *2000 MAIK "Nauka/Interperiodica".*

1. INTRODUCTION

Scanning near-field optical microscopy (SNOM) is a valuable research tool for imaging and investigating different samples with a subwavelength spatial resolution. The spatial resolution of SNOM is usually limited by the size of the aperture for light transmission and ranges from 50 to 100 nm, although a 20 nm resolution has been demonstrated [1, 2]. Further improvement of the resolution seems problematic for the "classical" SNOM configurations because the number of photons "seeping" through an aperture is rapidly decreasing with the decrease of the aperture size. A number of new approaches have been proposed recently to improve the resolution, such as the molecular exciton-based SNOM [3], apertureless SNOM [4], and SNOM using Fluorescence Resonant Energy Transfer (FRET) between a single fluorescence center of the tip and the sample under study [5].

In the latter case, the idea is based on the fact that when the distance between donor and acceptor molecules becomes smaller than the characteristic radius of a resonant energy transfer R_0 (which for typical donor–acceptor pairs ranges within 2–6 nm [6]), the probability of a dipole–dipole energy transfer between these molecules is close to unity (see, for instance, papers [6, 7] for a review). One should prepare the tip containing a single fluorescent center in the apex and scan it in close proximity to the sample surface (the relative distance should be smaller than R_0). If the donor fluorescent centers of the imaging tip are excited and the fluorescence of the acceptor centers of the sample is monitored (or vice versa), the spatial resolution will be governed not by the aperture size of the microscope but by the value of R_0. An analysis shows that not only the spatial resolution, but the sensitivity as well can be improved when using these FRET SNOMs [5, 8], which, of course, would be very important for the subsequent progress in the field.

The applicability of SNOM to detect a single molecule fluorescence is well established at present (see, e.g., recent reviews [9, 10] and references therein) and the possibility of the nondestructive scanning of the SNOM tips in the close proximity of the sample surface (in the contact mode) has been demonstrated [11, 12]. In this paper, we present the first experimental evidence of the applicability of FRET phenomena for near-field optical microscopy: a nanolocal resonant energy transfer process has been observed between two different dyes. One of them (the donor) has been deposited onto the glass sample surface and other (the acceptor) has been deposited onto the surface of a SNOM tip (sharpened optical fiber) or a standard AFM silicon nanotip. The FRET process has been realized only when the tip acquires a contact with the sample, i.e., in the regions with the sizes of only a few tens of nanometers, and it involves only thousands (or even hundreds) of dye molecules.

¶ This article was submitted by the authors in English.

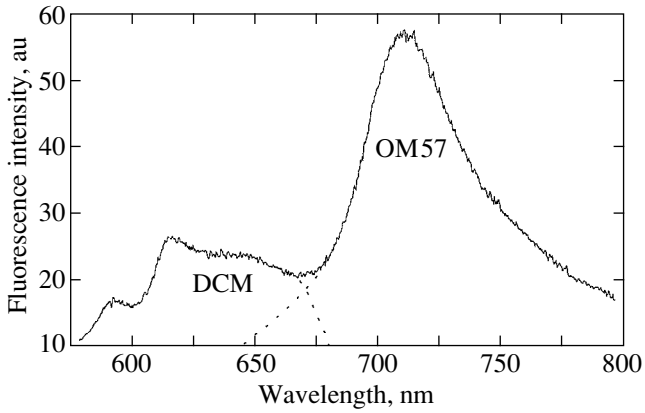

Fig. 1. Fluorescence spectrum of codeposited submonolayers of DCM and OM57 dyes.

A part of these results has been briefly discussed earlier in the letter [13]. A recent paper by Vickery and Dunn [14], where first images obtained with a FRET SNOM (without an analysis of the signal as a function of the tip-sample acting force) should also be mentioned in relation with the described problem.

2. SELECTION OF A DONOR–ACCEPTOR PAIR

A careful selection of a donor and acceptor dye molecule pair was necessary for the experiments described. When the laser excitation radiation wavelength is fixed (we have selected the 488 nm line of a cw argon ion laser), the donor molecules to be used should efficiently absorb this laser radiation and reemit light with a sufficiently large Stokes shift and a high quantum efficiency. The acceptor molecules to be used should efficiently absorb the photons reemitted by the donor, (i.e., good overlapping of the corresponding fluorescence and absorption spectra is required) and should also exhibit a high fluorescence yield with a large red shift with respect to the donor fluorescence. In addition, their direct excitation by the laser radiation should be minimal in order to diminish the background fluorescence and facilitate the observation of a nanolocal FRET phenomenon.

DCM dye molecules (4-dicyanomethilene-2-methyl-6-(p-dimethylaminoatyryl)-4H-pyran, number LC 6500 in Spectra Physics GmbH catalogue [15]) have been selected as donors because of their excellent fluorescent properties (the fluorescence quantum yield in solutions is close to unity, the absorption cross section value σ at the 488 nm wavelength is 6×10^{-17} cm^2) and high photostability.

Different dyes have been tested as acceptors. The best results have been obtained when using 1-butyl-3,3-dimethyl-2-[5-(1-butyl-3,3-dimethyl-3H-benz[e]indolin-2-yliden)-1,3-pentadienyl]-3H-benz[e]indolium perchlorate molecules (OM57 dye, Al'pha Akonis Company, Moscow): their absorption spectrum corresponds well to the fluorescence spectrum of DCM, and their absorption at the 488 nm wavelength is at least three orders of magnitude smaller than at the maximum; these molecules also have a reasonable fluorescence quantum yield (no smaller than 0.3) and photostability.

In Fig. 1, we present the spectrum of fluorescence of the two dyes, DCM and OM57, codeposited onto the same glass slide with the surface concentrations 3×10^{13} cm^{-2}. Such a concentration corresponds to a submonolayer coating: as known for Rhodamine dyes, one monolayer coating corresponds to the surface concentration $\sim 10^{14}$ cm^{-2} [16]. It is clear from this figure that under such conditions, the fluorescence of OM57 molecules (the spectral range 650–800 nm) is even more prominent than that of DCM (the spectral range 550–700 nm), keeping in mind that OM57 molecules do not absorb the excitation wavelength (the fluorescence spectrum of OM57 molecules, deposited in the same concentration but without DCM molecules on a glass slide, was orders of magnitude less intense and barely exceeded the noise level). Thus, this figure can be regarded as a demonstration of the dipole–dipole resonant energy transfer process between DCM and OM57 dye molecules on the surface.

For some other pairs of donor and acceptor molecules (DCM–DTDCI, DCM–HITCI, see [15] for the description of these dyes), the FRET process has been also observed but was not so prominent and the donor and acceptor fluorescence spectra were not so well resolved as for the DCM–OM57 pair. This is why we selected this particular pair of dyes for the subsequent experiments.

The characteristic radius R_0 of the resonance dipole–dipole energy transfer for this pair can be calculated using the well known relation [6, 7]

$$R_0 = \left(\frac{3}{4\pi}\int \frac{c^4}{\omega^4 n^4} F(\omega)\sigma(\omega)d\omega\right)^{1/6}, \qquad (1)$$

where $F(\omega)$ is the normalized fluorescence line shape of the donor and $\sigma(\omega)$ is the optical absorption cross section of the acceptor. From (1), it is easy to see that such a radius has a relatively slight dependence on the spectral overlapping integral (inverse sixth power only); calculations show that it ranges between 3 and 4 nm for all "reasonably overlapping" dye pairs, including DCM–OM57 (compare with the data given in [6]).

3. SCANNING NEAR-FIELD OPTICAL MICROSCOPE GEOMETRY

3.1. Experimental Equipment and Procedures

Different experimental schemes have been implemented for the demonstration of FRET phenomena in scanning probe microscopy. We start our discussion of the experimental results with the SNOM-based scheme where more quantitative results have been obtained.

The scheme of the experiment performed using the photon scanning tunneling (PSTM) version of SNOM [1, 2] is shown in Fig. 2. Two different homemade shear force-based SNOMs and homemade electronic units to

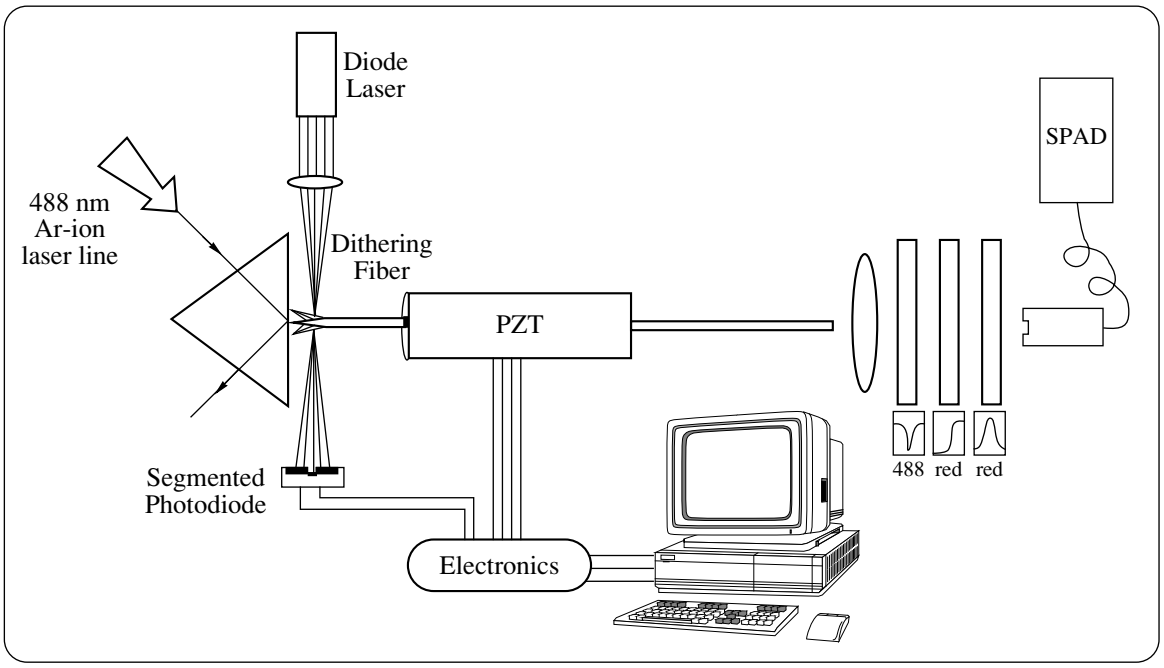

Fig. 2. Scheme of the PSTM-based FRET experiment.

control its performance have been used. In most of the experiments, the standard optical detection method to measure the amplitude of the lateral tip vibrations [1, 2] was utilized, but some critical experiments were performed using a non-optical shear force detection method similar to that described in [17]. We used SNOM tips with the curvature radius 100–200 nm prepared by the usual etching procedure of optical fibers in concentrated HF solutions [1, 2] or commercially available from Nanonics Supertips (Israel). Additional details about the construction of the microscopes used in the experiments can be found in [13, 18, 19].

To deposit the donor dye molecules onto the sample surface, we used the spin coating technique [20] as well as the simple method of spreading a small droplet (10 μl) of the dye solution onto the surface with the subsequent drying in air. No essential difference of the results has been observed.

Acceptor molecules have been deposited onto the surface of the SNOM tip. In this case, it seems essentially more difficult to elaborate the procedure to deposit the dye layers with a known and well-controllable concentration of the molecules: the complex shape of the tip, its very small size, and fragility make it impossible to use such well-established methods as the spin coating technique or long-time deposition of the sample inside a dye solution with the subsequent elimination of the excess solution by a tissue paper [21]. Thus the so-called withdrawal, or "dipping" approach seems to be the most suitable: the sharpened fiber tip is rapidly dipped into and extracted out of the dye solution; the thickness of the deposited film (and thus the surface concentration of dye molecules) is governed by fluid dynamics. The results of our experiments did not contradict the data known about the concentration dependence for flat surfaces [22, 23], and we are planning to finally clarify this point in future experiments.

The 488 nm spectral line of a cw argon ion laser was focused onto a glass prism surface under the conditions of total internal reflection (spot sizes were of the order 300 μm and the laser irradiation intensity I was 15 W/cm^2). Light coming out of the opposite side of the sharpened fiber was detected by a single photon avalanche diode (SPAD; EG & G, Canada, noise level 80 s^{-1}) after passing through a number of filters to suppress stray light and select the light originating from fluorescence of the acceptor molecules. The set of filters included a holographic notch filter for the 488 nm line, a red glass filter with the absorption edge of 660 or 695 nm, and interference filters centered at 750 nm with a width of 70 or 40 nm. It can be seen from Fig. 1 that such a set of filters enables the separation of the fluorescence coming from OM57 molecules from that coming from DCM molecules.

3.2. Results

In Fig. 3, we present the dependence of the fluorescence signal recorded by the EG & G SPAD for the case of DCM and OM57 molecules deposited with the surface concentrations 3×10^{13} cm^{-2} on the voltage driving the piezotube in the z-direction. Each point on this graph is a result of an average of 10–20 counts during one second each. The moment of contact between the tip and the sample was determined by the beginning of

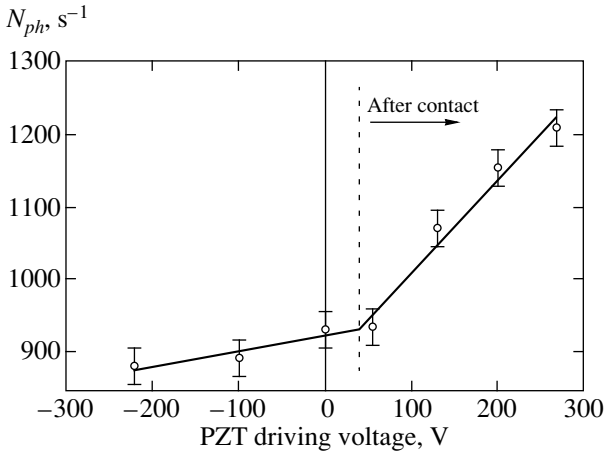

Fig. 3. The acceptor fluorescence signal dependence on the acting force recorded during the PSTM-based FRET experiment.

a decrease of the tip dithering amplitude as observed on an oscilloscope.

The distance between the tip and the sample, Δz, when out of contact, can be easily calculated as a function of the potential difference ΔU using the known calibration data for the driving piezo, $\Delta z = \zeta \Delta U$, where, $\zeta = 9.5$ nm V. After acquiring the contact, it is more reasonable to speak about the change in the force acting between the tip and the sample rather than about the change of a relative distance; an increase of the voltage tends to push the tip (rigidly fixed on the piezo) more strongly against the sample. The acting force F can be calculated using the spring constant k of the sharpened fiber by an obvious relation $F = k\zeta\Delta U$, and an action of this force leads to the flexural bending [12, 24, 25] and deformation of the tip.

From Fig. 3, it is easy to see that after acquiring the contact, the acceptor fluorescence signal starts to increase rapidly as the acting force increases. This effect has been well reproduced during at least a few tens of the cycles contact–out of contact measurements, but an overall slow decrease in the signal due to the photodegradation of the dyes was noticed.

A number of control experiments have been performed using the same tip-sample configuration but with the donor and acceptor dyes (either or one of or both them) absent. None of these control experiments revealed a behavior analogous to that presented in Fig. 3; only a very slow change in the fluorescence signal as a function of the driving voltage was usually observed and the contact point did not correspond to any peculiarities in the fluorescence signal. Of course, the absolute value of the recorded signal was smaller.

Similar results were obtained when we used another mode of SNOM operation, namely, the illumination mode SNOM (see Fig. 4) instead of the PSTM version described above. Donor dye molecules were deposited onto a thin glass slide surface. The SNOM tip, covered

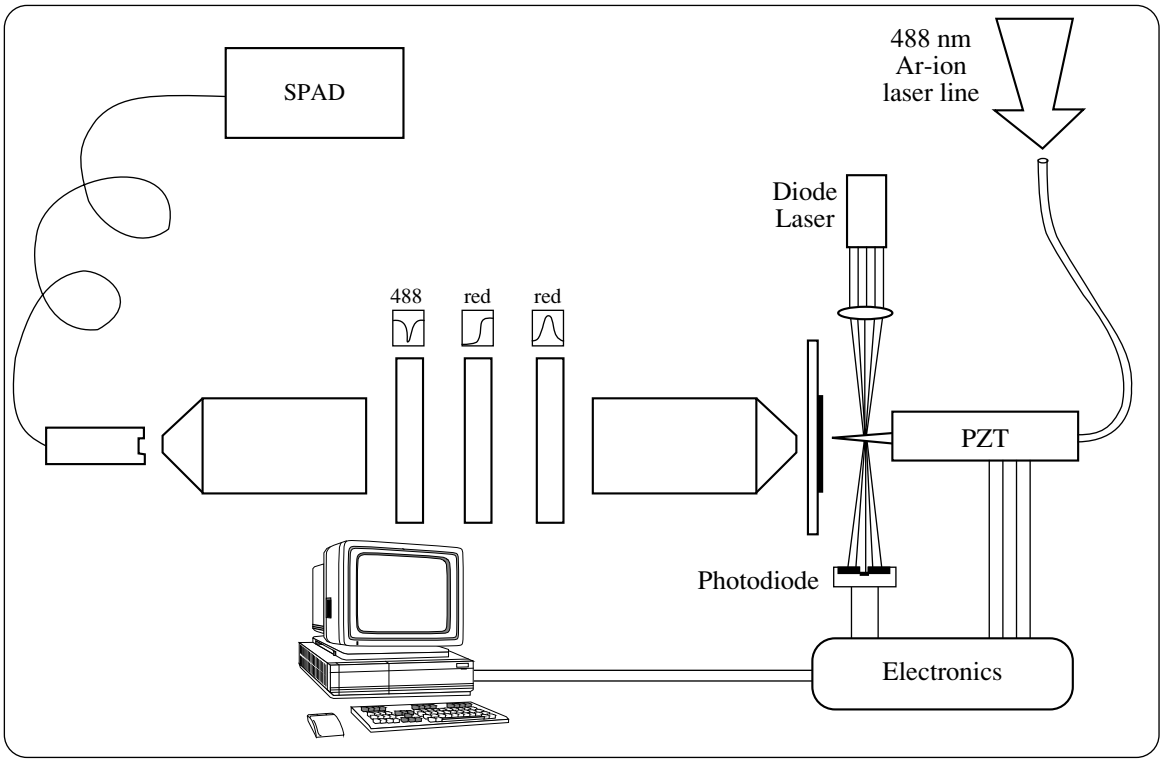

Fig. 4. Scheme of the illumination mode SNOM-based FRET experiment.

with a OM57 acceptor molecule layer, was used as a light source. The same detector and combination of filters were used. As in the previous case, the OM57 fluorescence signal drastically increased after the acquisition of the contact only when both dye layers were present.

3.3. Discussion

Thus, the acceptor fluorescence signal behavior presented in Fig. 3 is definitely due to the presence of both dyes and should be regarded as a demonstration of FRET phenomena in scanning-probe microscopy. The increase of the fluorescence signal as a result of the increase of the acting force was due to the corresponding increase of the contact surface and thus, of a number of molecules involved in the energy transfer process.

Semiquantitatively, the experimental data can be described as follows. Experimental measurements of the spring constant k for the glass fiber tips [11] as well as calculations based on the mechanical properties of the flexural bending of a glass cone [24] show that for a tip with the curvature radius 100 nm, the spring constant should be of the order 500–1000 N/m. This means that for an equivalent displacement of the piezo, $\zeta\Delta U$, (maximum value attains 1.9 μm) the acting force value should range within 10^{-4}–10^{-3} N. (Note that a similar range of forces was used in the recent SNOM experiments using normal dithering of a tip [12, 24]. Under the action of such a force, the tip will exhibit flexural bending [24, 25] and elastic deformation. Both these processes will result in an increase of the contact surface. For a rough estimate of the elastic deformation, one can use the known Hertzian expression to describe the contact radius r_c of a sphere pressed against a flat sample surface as a function of the acting force F (see, for example, [18], where the problem of elastic deformations in AFM has been specially investigated:

$$r_c = \left(\frac{3(1-\nu^2)Fr}{4E}\right)^{1/3}. \qquad (2)$$

Here r is the curvature radius of the tip, $E = 7 \times 10^{10}$ N/m^2 and $\nu = 0.25$ are typical Young modulus and Poisson ratio for glass. For $F = 10^{-4}$ N, r = 100 nm, this expression gives $r_c = 46$ nm, which corresponds to $N_1 \sim 2000$ molecules in the "FRET active" contact area for the surface concentration 3×10^{13} cm^{-2}.

An absolute value of the fluorescence signal recorded for the sharpest tips used was equal to N_{ph} = 80–100 s^{-1} (with the signal to noise ratio of the order of unity). Knowing this value, we can estimate the number of molecules N_2 contributing to the measured signal using the simple relation

$$N_2 = \frac{N_{ph}h\nu}{I\sigma\eta\Phi}, \qquad (3)$$

where $h\nu = 4.07 \times 10^{-19}$ J is the photon energy, Φ is the fluorescence quantum yield of the acceptor molecule, and η is an overall efficiency of the photon collection and detection for our experimental system. The latter can be estimated as follows. The efficiency of the fluorescence photon collection by a sharpened fiber for a geometry similar to ours was reported to be $2–5 \times 10^{-3}$ [26]. We estimate the efficiency of the detection of photons coming out of the fiber about 0.1–0.05 (this value is mainly due to the registration only within a rather narrow spectral band of the total acceptor fluorescence because of the strong filtering, see above) and thus, the overall efficiency of the detection is $1–5 \times 10^{-4}$. This means that $N_2 \sim$ 300–1500 acceptor molecules contribute to the measured signal (we assume $\Phi = 0.3$). Both N_1 and N_2 values are in reasonable coincidence with each other, which strengthens our conclusions about an observation of the "nanolocal" FRET phenomenon with only hundreds to thousands of molecules involved.

4. ATOMIC FORCE MICROSCOPE GEOMETRY

The above results were qualitatively confirmed in another series of experiments performed with the same DCM–OM57 dye pair. OM57 acceptor molecules were deposited onto the surface of a silicon tip of a standard AFM cantilever (NT–MDT, Moscow, the force constant 0.12 N/m, the curvature radius of the tip 10–20 nm). DCM donor molecules were deposited onto a thin glass slide surface and a 488 nm laser line was focused onto this surface by a 40× microobjective after a reflection from a selective mirror at the angle of 45° (see Fig. 5). Contact between the AFM tip and the sample as well as the acting force was controlled by monitoring the reflection of a focused diode laser radiation from the opposite side of the cantilever, as is typical in the usual contact mode AFM. The same driving piezo and electronic control unit as in the SNOM-based experiment described above were used. Fluorescent light was collected using the same 40 x microobjective, and after the passage through the selective mirror without reflection, it was refocused onto the entrance slit of a CCD-camera-equipped monochromator. The same set of filters as described earlier (except for an interference filter centered at 750 nm) was used. Light intensity was essentially higher, ~600 W/cm^2, and as a result, the photodegradation was more prominent. Nevertheless, it was possible to observe the difference between the "contact" and "noncontact" fluorescence during a number of the cycles contact-out of contact measurements (analogous to the SNOM experiments described above).

No quantitative information has been collected in these series of experiments, but in Fig. 6, we present two fluorescence spectra recorded when in deep contact (1) and out of contact (2). The acting force, estimated for the "deep contact" case in the same manner as discussed above for the SNOM case, was equal to ~10^{-6} N. It can be clearly seen that the signal obtained while in

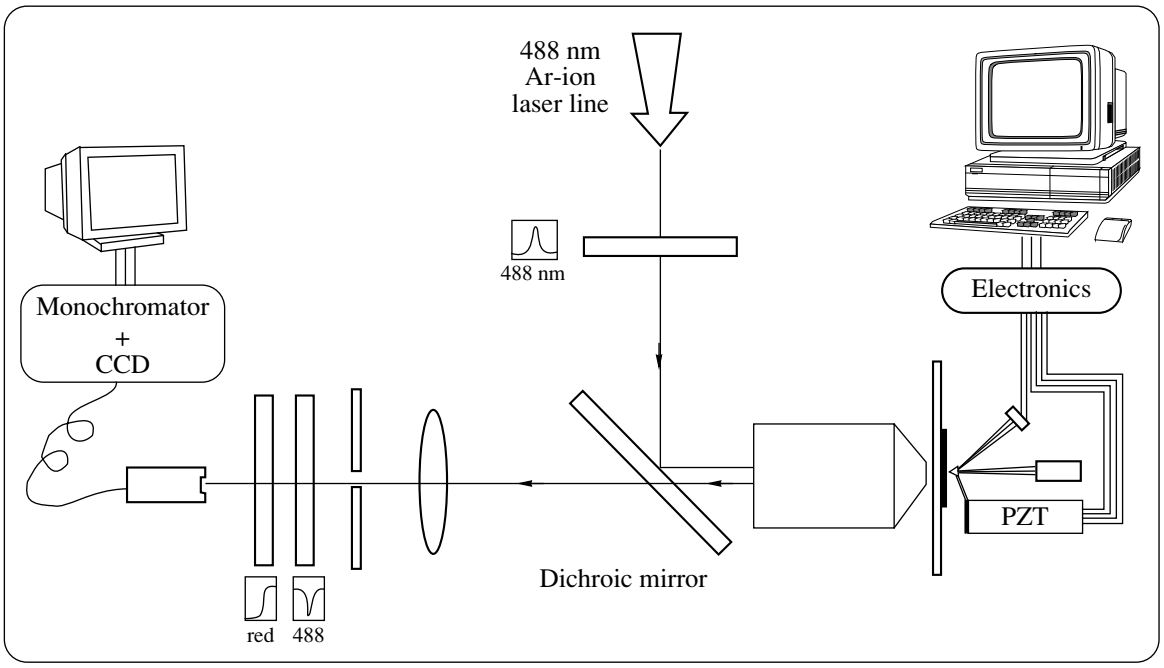

Fig. 5. Scheme of the AFM-based FRET experiment.

contact was 10–20% larger than that obtained out of contact. This effect was not observed in control experiments, when both or one dye were missing, which is an additional indication of the observation of the AFM- (or SNOM-) related nanolocal FRET phenomenon.

5. FLUORESCENCE RESONANCE ENERGY TRANSFER PROBE MICROSCOPE

The results presented in this work should be treated as a demonstration of the FRET phenomenon in scanning near-field optical microscopy and atomic force microscopy techniques. Of course, the difference between SNOM and AFM is rather arbitrary in this context: for example, silicon AFM levers similar to those described in Section 4 are optically semitransparent and optical near-field microscopy can be implemented to measure the light passing through these levers [27]. An important point is that we succeeded in recording a nanolocal "contact dependent" fluorescence signal corresponding to a few thousands or even hundreds of FRET-active molecules. Relying on the obtained experimental data. Sensitivity, noise level, etc., we believe that using a slightly modified approach (for example, that based on an illumination-geometry SNOM, where single fluorescent molecules were indeed observed recently [9, 10]), it will be possible to observe the FRET phenomenon at the level of only one single molecule.

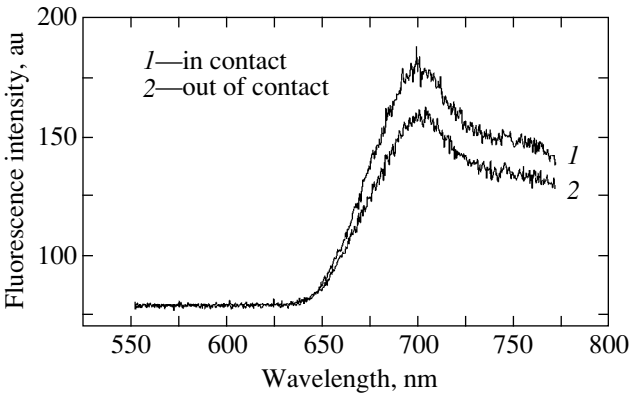

Fig. 6. Fluorescence signals recorded during the AFM-based FRET experiment for the tip in contact (curve *1*) and out of contact (curve *2*) with the sample.

Thus, based on the experimental results already obtained, we believe that it is now the time to briefly discuss a FRET probe Microscope that is under construction in our laboratory (Troitsk). The particular scheme of this microscope is presented in Fig. 7. The principal element of the FRET probe is a small polystyrene bead stained with a dye. Such microspheres are commercially available in a broad range of sizes (10 μm–20 nm) and dyes and are routinely used in the optical fluorescent microscopy as markers (see, e.g., [28]). Preliminary results indicating FRET processes involving some dye doped beads commercially available from Molecular Probes, Oregon, have been recently obtained in our laboratory (Lausanne: unpublished), but one should be sure that the dye molecules at the surface are not covered by protective layers.

To provide the possibility of the probe manipulation, we are elaborating the method to fix it to the apex of a microcapillary, as indicated in Fig. 7. Fixing may

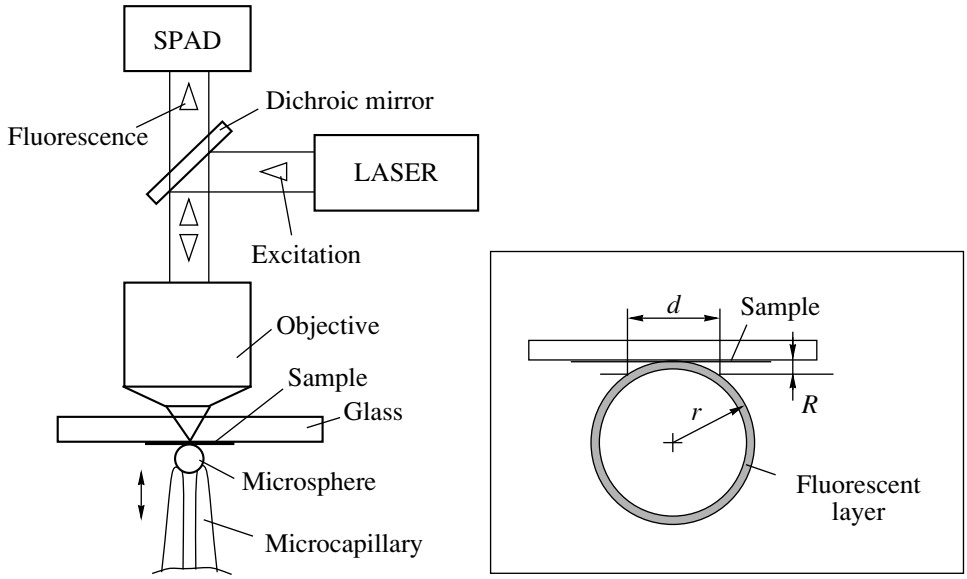

Fig. 7. Scheme of a FRET probe microscope. Only the upper part of the capillary is shown. The glass slide with the sample is supposed to be moved by a scanner of the microscope. The electronic part (not shown) is similar to that of a scanning probe microscope.

be possible relying on the van-der-Waals forces or a specific chemical binding, and a number of microcapillaries with the diameter ranging from 100 nm to a few microns is now commercially available.

The optical scheme of the FRET probe microscope is similar to that of the confocal fluorescent microscope. The laser beam is reflected from a dichroic mirror and is focused on the sample. Let us assume that the sample contains donor molecules and the bead contains acceptor dye molecules. If the donor–acceptor pair is chosen as described above, mainly the donor molecules are excited due to the FRET process. The light from fluorescent acceptor molecules is collected by the same objective that is used for illumination of the sample. The light coming through the dichroic mirror is detected by a SPAD or a PMT.

The possibility to modulate the probe-sample distance is implemented in the microscope construction. This enables one to improve the sensitivity and to remove the background signals caused by "tails" of donor fluorescence and the direct excitation of acceptor molecules. The modulation allows the distance-dependent part of the signal to be extracted, because the FRET between the probe and the sample is possible only when the bead comes in contact with the sample. The modulation in the range of several tens of nanometers will suffice because the Förster radius does not exceed several nanometers [6], and such a modulation can be realized based on the usual shear force feedback [1, 2] or normal tip vibrations that we have recently realized [12, 24].

A simple estimation of the lateral resolution of the microscope can be made from elementary geometrical considerations. If we model the sphere as touching the surface without elastic deformation (see insert in Fig. 7), the FRET is possible for acceptor molecules located between the surface and the imaginary plane at the distance R_0 (Förster radius) from the surface, one should now distinguish between two different situations: i) there is only one acceptor molecule inside this area, and ii) there are several molecules inside it. In the former case, the resolution is governed by the Förster radius [5]. Note that this is exactly the case for the commercially available beads with the diameter $2r = 20$ nm (Molecular Probes, Oregon). Such a bead contains $N \sim 180$ molecules of the dye distributed in the volume of the sphere (not the surface) [28], and therefore, we can find

$$n \approx (1/2)N(R_0/r)^3 \approx 0.7$$

acceptor molecules in the FRET-active area (we take the Förster radius R_0 equal to 2 nm). Indeed, it is not necessary to use the smallest available spheres with the diameter 20 nm to attain such a resolution. Similar numbers can be obtained for much large beads: applying the same relation for $2r = 1$ μm and $N = 1.3 \times 10^7$ [28] gives $n = 0.4$.

In the latter case, the resolution is determined by the diameter d of the interaction zone. Taking into account that the radius of the sphere $r \gg R_0$, it is easy to find that $d \approx 2\sqrt{2rR_0}$, which corresponds to the resolution $d \approx 12$ nm for the beads with $2r = 20$ nm. An important issue is the number N of interacting molecules in the bead. The area of the bead surface inside the diameter d is defined by the expression

$$2\pi r^2\left(\sqrt{1-\frac{d^2}{4r^2}}\right).$$

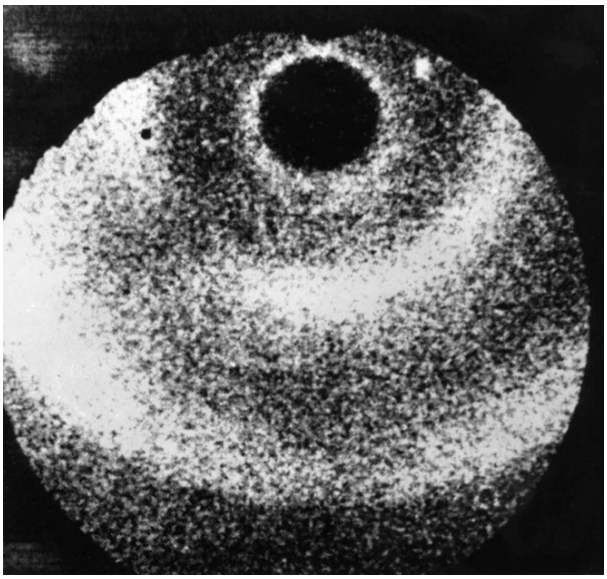

Fig. 8. The field emission image of the borosilicate glass microcapillary with the inner diameter of 0.5 μm. The image of the central hole is shifted to the upper part of the figure. The thickness of walls looks exaggerated due to the peculiarities of image formation in the field emission microscope.

For an estimate, an approximation gives simply $S = \pi d^2/4$. If the surface density of dye molecules is $n = 10^{14}$ cm^{-2} (beads having dye molecules on the surface can be easily prepared in the laboratory), we have $N = nS \approx 270$ molecules, which is large enough to avoid the photostability problem, which is crucial at the single-molecule level.

We emphasize that the resolution 10–20 nm can be achieved without the subwavelength aperture that is a principal element of the standard near-field microscope. Complex boundary conditions for the near-field at the probe apex of SNOM considerably complicate the analysis of SNOM images which can lead to a number of artifacts (see, e.g., [29]). The FRET probe microscope is free from these drawbacks because of the absence of the aperture and the physical clarity of the interaction.

6. CONCLUSIONS

In this paper, we have presented experimental results concerning an observation of nanolocal FRET processes for the usually used SNOM and AFM geometries; we then discussed the FRET probe microscope currently under construction in Troitsk. In addition, practical elaboration of this FRET microscope is especially timely because we have at our disposal the already finished one-atom fluorescent tips made of LiF : F_2 crystal fragments, where only one effective and very photostable fluorescent center in the tip apex region (F_2 aggregate center, which is the specific defect of LiF crystalline lattice) has been observed using the laser selective photoelectron projection microscopy technique [8, 30]. We used the same technique to observe the apex of the nanocapillary currently explored in the FRET probe microscope under construction (see Fig. 8), and will use it to control the fixing of a dye-saturated bead on the capillary apex, as described in Section 5.

The practical realization of the FRET probe microscope makes it possible to drastically improve the spatial resolution and the sensitivity of scanning near-field optical microscopy, thereby opening new prospects in the field [5, 8]. The FRET SNOM will be very useful when working not only at the single-molecule level, but also with hundreds or thousands of molecules involved (exactly as reported here), because this approach, in any case, improves the resolution and sensitivity of SNOM and enlarges the number of possible experimental schemes of the microscope to be used.

ACKNOWLEDGMENTS

This research was supported by the Swiss National Science Foundation (grants nos. 20-50427.97, 20-57133.99 and 21-50805.97) and Russian Department of Physics and Technology (grant no. 3-1).

REFERENCES

1. *Near Field Optics*, Ed. by D. W. Pohl and D. Courjon (Kluwer, Dordrecht, 1993).
2. M. A. Paesler and P. J. Moyer, *Near Field Optics: Theory, Instrumentations, and Applications* (Wiley, New York, 1996).
3. R. Kopelman and W. Tan, Appl. Spectrosc. Rev. **29**, 39 (1994).
4. F. Zenhausern, M. P. O'Boyle, and H. K. Wickramasinghe, Appl. Phys. Lett. **65**, 1623 (1994).
5. S. K. Sekatskiĭ and V. S. Letokhov, Pis'ma Zh. Éksp. Teor. Fiz. **63**, 323 (1996) [JETP Lett. **63**, 319 (1996)].
6. P. Wu and L. Brandt, Anal. Biochem. **218**, 1 (1994).
7. V. M. Agranovitch and M. D. Galanin, *Electron Excitation Energy Transfer in Condensed Matter* (North-Holland, Amsterdam, 1982).
8. S. K. Sekatskiĭ and V. S. Letokhov, Appl. Phys. B **63**, 525 (1996).
9. W. E. Moerner and M. Orrit, Science **283**, 1670 (1999).
10. S. Weiss, Science **283**, 1676 (1999).
11. C. E. Talley, G. A. Cooksey, and R. C. Dunn, Appl. Phys. Lett. **69**, 3809 (1996).
12. D. A. Lapshin, S. K. Sekatskiĭ, V. S. Letokhov, and V. N. Reshetov, Pis'ma Zh. Éksp. Teor. Fiz. **67**, 243 (1998) [JETP Lett. **67**, 263 (1998)].
13. G. T. Shubeita, S. K. Sekatskiĭ, M. Chergui, *et al.*, Appl. Phys. Lett. **74**, 3453 (1999).
14. S. A. Vickery and R. C. Dunn, Biophys. J. **76**, 1812 (1999).
15. U. Brackmann, *Lambdachrome Laser Dyes* (Lambda Physics, Göttingen, 1997).
16. D. C. Nguen, R. E. Muenchausen, R. A. Keller, and N. S. Nogar, Opt. Commun. **60**, 111 (1986).

17. A. Drabenstedt, J. Wrachtrup, and C. von Borczyskowski, Appl. Phys. Lett. **68**, 3497 (1996).
18. M. Heuberger, G. Dietler, and L. Schlapbach, Nanotechnology **5**, 12 (1994).
19. D. A. Lapshin, Zh. Tekh. Fiz. **68** (9), 51 (1998) [Tech. Phys. **43**, 1055 (1998)].
20. M. Lieberherr, C. Fattinger, and W. Lukosz, Surf. Sci. **189–190**, 954 (1987).
21. H. Gerischer and F. Willig, Top. Curr. Chem. **61**, 31 (1976).
22. S. Garoff, R. B. Stephens, C. D. Hanson, and G. K. Sorensen, Opt. Commun. **41**, 257 (1982).
23. C.-C. Yang, J. E. Josefowicz, and L. Alexandru, Thin Solid Films **74**, 117 (1980).
24. D. A. Lapshin, V. N. Reshetov, S. K. Sekatskiĭ, and V. S. Letokhov, Ultramicroscopy **76**, 13 (1999).
25. P. K. Wei and W. S. Fann, J. Appl. Phys. **84**, 4655 (1998).
26. M. Ohtsu, J. Lightwave Technol. **13**, 1200 (1995).
27. H. U. Danzenbrink, A. Castiaux, C. Girard, *et al.*, Ultramicroscopy **71**, 371 (1998).
28. R. P. Haugland, *Handbook of Fluorescent Probes and Research Chemicals* (Molecular Probes, Eugene, Oregon, 1997).
29. B. Hecht, H. Bielefeldt, Y. Innouye, *et al.*, J. Appl. Phys. **81**, 2492 (1997).
30. S. K. Sekatskiĭ and V. S. Letokhov, Pis'ma Zh. Éksp. Teor. Fiz. **65**, 435 (1997) [JETP Lett. **65**, 465 (1997)].